

Bethe-lattice calculations for the phase diagram of a two-state Janus gas

Danilo B. Liarte

E-mail: danilo@if.usp.br

Institute of Physics, Caixa Postal 66318, CEP 05314-970, São Paulo, SP, Brazil

Silvio R. Salinas

E-mail: ssalinas@if.usp.br

Institute of Physics, Caixa Postal 66318, CEP 05314-970, São Paulo, SP, Brazil

January 2015

Abstract. We use a simple lattice statistical model to analyze the effects of directional interactions on the phase diagram of a fluid of two-state Janus particles. The problem is formulated in terms of nonlinear recursion relations along the branches of a Cayley tree. Directional interactions are taken into account by the geometry of this graph. Physical solutions on the Bethe lattice (the deep interior of a Cayley tree) come from the analysis of the attractors of the recursion relations. We investigate a number of situations, depending on the concentrations of the types of Janus particles and the parameters of the potential, and make contact with results from recent numerical simulations.

1. Introduction

The production and characterization of solutions of Janus particles, whose spherical surface is divided into hydrophobic and hydrophilic hemispheres, have attracted the attention of a number of authors [1, 2, 3, 4, 5, 6]. Studies of the behavior of these colloidal systems must take into account that Janus particles interact in a different way depending on their relative orientations. A simple form of a pairwise directional potential has been proposed by Kern and Frenkel [7], who introduced a model of hard spheres with the addition of a square-well potential with directional attractive short-range interactions. The Kern-Frenkel model has been used in several analytical and numerical investigations (see e.g. [8, 9, 4, 6]). In particular, a simplified two-state version of the Kern-Frenkel model, which is reminiscent of the Zwanzig approximation for liquid-crystalline models, and can be experimentally realised by the application of an electric field, has been extensively studied in [10, 11].

These recent calculations provided the motivation to introduce a simple lattice statistical model to analyze the effects of directional interactions in a Janus gas of

particles. It is well-known that lattice gas models on the Bethe lattice, which is the deep interior of a large Cayley tree, lead to the same (analytic) equations of state of the quasi-chemical approximation for a simple lattice gas [12]. In the limit of infinite coordination of the tree, it has been shown that one regains the usual mean-field solutions [13, 14]. We then revisit the lattice gas problem on a Cayley tree with the inclusion of directional interactions. We consider a mixture of Janus particles of types a and b , with hydrophobic (hydrophilic) hemispheres in the upper (lower) half part of their respective spherical surfaces, which amounts to considering a two-state, Ising-like, representation of a Janus gas (see figure 1). In a grand canonical formulation, we add a chemical potential to control the density of each type of particle. Taking advantage of the geometrical structure of this tree, it becomes particularly simple to introduce directional interactions between first-neighbor sites along the branches of the graph. We choose the parameters of the potential, and the concentration of the two types of particles, to make contact with the available numerical simulations.

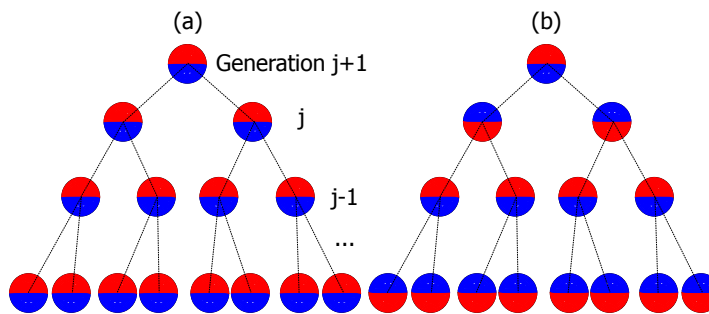


Figure 1. Sketch of some generations of a Cayley tree of ramification $r = 2$. The two-state system is formed by Janus particles of type a (depicted as circles with red heads up in this figure) and of type b (blue heads up). The trees on the left (a), and on the right (b), illustrate macroscopic configurations with a high density of a -particles, and a modulated (“striped”) phase, respectively.

This article is organized as follows. In Section I, we describe the lattice statistical model on a Cayley tree. We show that the solutions on the Bethe lattice (deep in the interior of the tree) can be obtained from the analysis of the recursion relations associated with a nonlinear discrete map. In sections II and III, we analyze some particular cases, and make contact with results from simulations. In particular, we show that attractive interactions of the Kern-Frenkel form lead to layered modulated structures, which have indeed been found in the simulations [11]. Although we do not make quantitative contacts with the simulations, we do claim to have used a much simpler approach to obtain a number of analytical qualitatively results, for a full range of model parameters. In particular, we provide a unified view of the phase transitions described by a “cubic diagram” of interaction parameters drawn by Fantoni and collaborators [11].

2. Formulation of the problem on the Bethe Lattice

We consider Janus particles restricted to two orientations. These particles are represented by a set variables $\{t_i\}$, on the sites of a tree, so that $t_i = 1$ is associated with a particle of type a on site i , and $t_i = 0$ represents a Janus particle of type b on site i . The pair interaction energy between nearest-neighbor sites i and j along the branches of the tree is given by

$$E_{ij} = -(\epsilon_{aa} + \epsilon_{bb} - \epsilon_{ab} - \epsilon_{ba})t_i t_j - (\epsilon_{ab} - \epsilon_{bb})t_i - (\epsilon_{ba} - \epsilon_{bb})t_j - \epsilon_{bb}. \quad (1)$$

Note that aa and bb particles interact with energies $-\epsilon_{aa}$ and $-\epsilon_{bb}$, respectively. Also, note that ab and ba particles interact with (in general) different energies, $-\epsilon_{ab} \neq -\epsilon_{ba}$. Of course, if $\epsilon_{ab} = \epsilon_{ba}$ we regain the results for a usual lattice gas representation of a binary liquid mixture [12].

In the appendix, we use standard treatments for a Cayley tree [14], in order to obtain the recursion relations

$$\Xi_{j+1}^a = z \left[e^{K_{aa}} \Xi_j^a + e^{K_{ab}} \Xi_j^b \right]^r \quad (2)$$

and

$$\Xi_{j+1}^b = \left[e^{K_{ba}} \Xi_j^a + e^{K_{bb}} \Xi_j^b \right]^r, \quad (3)$$

for the partial grand partition function Ξ_j^a (Ξ_j^b) that is associated with the sub-tree generated by a site at generation j which is occupied by a particle of type a (b). $K_{kl} = \beta \epsilon_{kl}$, for $k, l = a, b$, $\beta = 1/k_B T$ is the inverse temperature, $z = \exp(\beta \mu)$ is the fugacity, and μ is the chemical potential (associated with particles of type a). It is now convenient to define the density of particles of type a in generation j ,

$$\rho_j = \frac{\Xi_j^a}{\Xi_j^a + \Xi_j^b}, \quad (4)$$

so that Eqs. (A.3) and (A.4) may be written as a single recursion relation

$$\rho_{j+1} = f(\rho_j), \quad (5)$$

with

$$f(x) = \left\{ 1 + z \left[\frac{e^{K_{ba}} x + e^{K_{bb}} (1-x)}{e^{K_{aa}} x + e^{K_{ab}} (1-x)} \right]^r \right\}^{-1}, \quad (6)$$

where $0 \leq x \leq 1$. This is the central result of this formulation. At this point the problem is reduced to analyzing the general map given by Eq. (5), from which we obtain the main features of the phase diagrams in terms of temperature, $T = 1/(k_B \beta)$, and chemical potential μ (and with different choices of the energy parameters).

It is interesting to investigate the limit of infinite coordination of the tree, $r \rightarrow \infty$, with fixed values $r\epsilon_{aa}$, $r\epsilon_{bb}$, $r\epsilon_{ab}$, and $r\epsilon_{ba}$. In this limit, it is easy to show that

$$f(x) \rightarrow f_\infty(x) = \left(1 + e^{K_1 + K_2 x} \right)^{-1}, \quad (7)$$

where

$$K_1 = \beta (\mu + \delta), \quad K_2 = \beta \Delta, \quad (8)$$

with

$$\Delta = r(\epsilon_{ab} + \epsilon_{ba} - \epsilon_{aa} - \epsilon_{bb}), \quad \delta = r(\epsilon_{bb} - \epsilon_{ab}). \quad (9)$$

This limit is known to lead to the solutions for an analogous fully-connected, mean-field model [13, 14]. It is important to remark that the phase diagrams depend on just two parameters, K_1 and K_2 , and that the parameter Δ plays a quite special role.

At high temperatures, both $f(x)$ and $f_\infty(x)$ tend to $1/2$, so that $\rho \rightarrow 1/2$ as $T \rightarrow \infty$. At low temperatures, there are two possible scenarios depending on the sign of Δ . If $\Delta < 0$, there is a discontinuous (first-order) line of transitions in a diagram in terms of chemical potential and temperature. This border, which separates states with low- and high-density of particles of type a , ends at a critical point. In the second scenario, for $\Delta > 0$, the analogous phase diagram displays a critical line enclosing a cycle-2 periodic phase. This approach provides a unified view of the phase transitions described by the choice of interaction parameters according to the cubic diagram of Fantoni and collaborators (see table 1). Except for the HS and SW models, which are non-interacting models in our lattice approach, all of the cases in this diagram are shown to fit into one of these two scenarios. Also, although the finite-coordination map is more respectable than the mean-field limit, we find no qualitative changes for trees with ramification $r > 1$ ($r = 1$ corresponds to a one-dimensional model, which has no phase transition at finite temperature). We will discuss these points in the following sections.

Model	ϵ_{aa}	ϵ_{ab}	ϵ_{ba}	ϵ_{bb}	Δ
HS	0	0	0	0	0
A0	0	ϵ	0	0	$r\epsilon$
I0	ϵ	0	0	ϵ	$-2r\epsilon$
J0	0	ϵ	ϵ	0	$2r\epsilon$
B0	ϵ	ϵ	0	ϵ	$-r\epsilon$
SW	ϵ	ϵ	ϵ	ϵ	0

Table 1. Definition of the models and corresponding values of Δ according to nomenclature defined in [11].

3. Discontinuous transition ($\Delta < 0$)

We first consider a simple case, $\epsilon_{aa} = \epsilon_{bb} = \epsilon/r > 0$, $\epsilon_{ab} = \epsilon_{ba} = 0$, which corresponds to I_0 in the cubic representation of Fantoni and collaborators [11]. The attractors of the map can be visualized if we draw graphs of $f(\rho)$, given by Eq. (6) in terms of ρ , as shown in figure 2, for a fixed temperature ($k_B T/\epsilon = 0.3$), a given ramification of the tree ($r = 5$), and for several values of the chemical potential ($\mu/\epsilon = -0.4, -0.17, 0, 0.17$ and 0.4). Fixed points are solutions of the equation $f(\rho) = \rho$, so that we plot ρ as the black dotted line in this figure. These plots cover all the three qualitatively

distinct behaviors of the map for $\Delta < 0$. There can be a single stable fixed point (black curves), a stable and a marginally stable fixed point (blue curves), and two stable and one unstable fixed points (red curve). The plots suggest a first-order transition from a high to a low density phase of a -particles. The blue curves indicate the emergence (or vanishing) of two fixed points, as well as their stability threshold. In a phase diagram in terms of temperature and chemical potential, the blue curves describe the behavior of the map along the spinodal lines. The red curve shows the behavior of the map at the transition (in the next paragraph, we show that, below a certain critical temperature, there is a first-order phase transition at $\mu = |\Delta|/2 - \delta$, with $\mu = 0$ in the I_0 case of the cubic diagram). A numerical inspection of Eqs. (5) and (6) leads to no additional characteristic structures of the map.

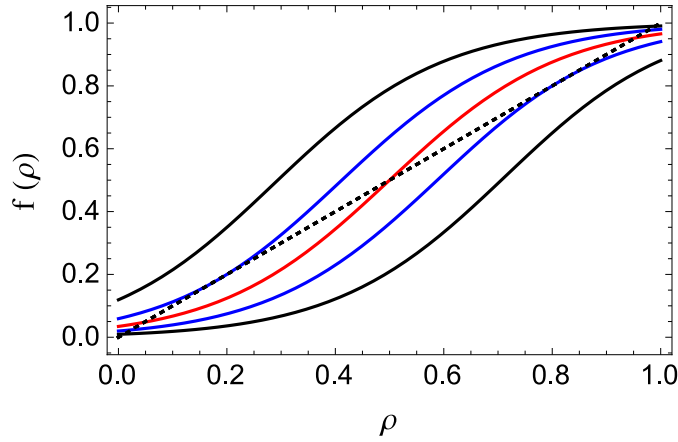


Figure 2. Plots of $f(\rho)$ for $\Delta < 0$. We assume temperature $k_B T/\epsilon = 0.3$, ramification $r = 5$, and several values of the chemical potential, $\mu/\epsilon = -0.4; -0.17; 0; 0.17; \text{ and } 0.4$ (with ordered curves from left to right, for increasing values of μ). The black dotted line corresponds to ρ .

In figure 3, we draw some phase diagrams in terms of $(\mu + \delta)/|\Delta|$ and $k_B T/|\Delta|$ for a tree of finite coordination ($r = 5$) and at the infinite coordination limit. There is a critical point at $(\mu_c + \delta)/|\Delta| = 1/2$, and $k_B T_c/|\Delta| = 1/4$. The black solid line, for $(\mu + \delta)/|\Delta| = 1/2$, and $k_B T/|\Delta| < 1/4$, is a first-order boundary. The spinodal limits, which are represented by the dashed lines, are given by the equations

$$x_0 = f(x_0), \quad |f(x_0)| = 1. \quad (10)$$

In the infinite-coordination limit, we have the set of parametric equations

$$\frac{k_B T}{|\Delta|} = \rho(1 - \rho), \quad (11)$$

and

$$\frac{(\mu + \delta)}{|\Delta|} = \rho(1 - \rho) \ln \frac{1 - \rho}{\rho} + \rho, \quad (12)$$

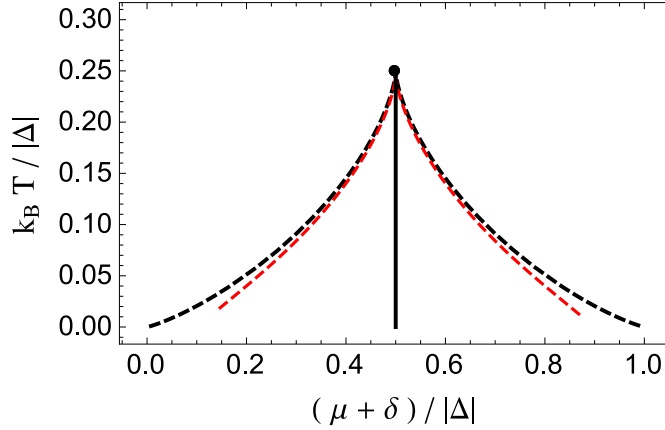


Figure 3. Phase diagram (temperature versus chemical potential) for $\Delta < 0$. The solid black line of first-order transitions ends at a critical point. We also show spinodal lines (dashed) for a tree of finite coordination (red lines) and in the mean-field limit (black lines).

with $0 \leq \rho \leq 1$. In order to describe the first-order boundary, we note that, at a fixed point of f_∞ , we have

$$(\mu + \delta)/|\Delta| = \rho + \frac{k_B T}{|\Delta|} \ln \frac{1 - \rho}{\rho}. \quad (13)$$

Therefore, $(\mu + \delta)/|\Delta| - 1/2$ is an odd function of $\rho - 1/2$, so that

$$\left| \int_{\rho_1}^{1/2} [(\mu + \delta)/|\Delta| - 1/2] d\rho \right| = \left| \int_{1/2}^{1-\rho_1} [(\mu + \delta)/|\Delta| - 1/2] d\rho \right|, \quad (14)$$

where ρ_1 is the smallest solution of $(\mu + \delta)/|\Delta| = 1/2$. If we resort to a Maxwell construction [14], this leads to a first-order boundary, given by $(\mu + \delta)/|\Delta| = 1/2$. Along this border, using Eq. (13), we have

$$\frac{k_B T}{|\Delta|} = \frac{1}{2} \frac{1 - 2\rho}{\ln \frac{1 - \rho}{\rho}}, \quad (15)$$

so that the two coexistent densities are the solutions $(\rho, 1 - \rho)$ of Eq. (15), with $0 \leq \rho \leq 1$, and converge to $\rho \rightarrow 1/2$ at $T_c = |\Delta|/4k_B$. In figure 4, we show the coexistence curve (black solid curve) and a few tie lines (in blue) in the mean-field limit. We also show isotherms of the chemical potential (red dotted curves), which are adequately scaled with temperature so that the corrected solutions, according to Maxwell's construction, correspond to the coexistence tie lines. Similar graphs and results can be numerically obtained for trees of finite coordination (with $q \geq 2$). The cases I_0 and B_0 in the cubic diagram of parameters are fully understood according to the general behavior displayed in figures 3 and 4.

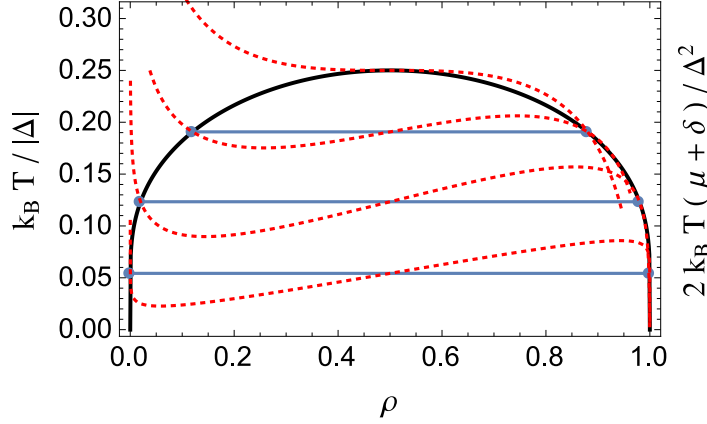


Figure 4. The black solid line is a coexistence curve (temperature versus concentration of particles of type a). We also show tie lines (blue), and isotherms (red dotted lines) for the chemical potential in the mean-field limit.

4. Continuous transition ($\Delta > 0$)

For $\Delta > 0$, at low temperatures, instead of a first-order boundary, there is a critical line from a disordered to a cycle-2 periodic phase. We first sketch the properties of the map in the simple A_0 case of the cubic diagram of interactions, with $\epsilon_{ab} = \epsilon/r > 0$, and $\epsilon_{aa} = \epsilon_{bb} = \epsilon_{ba} = 0$. Now there are only two scenarios. The map has either a single stable fixed point or one unstable fixed point and a stable cycle of period 2. In figure 5a, we draw ρ (dotted line), $f(\rho)$ (dashed lines), and $f \circ f(\rho)$ (solid lines), for fixed chemical potential, $\mu/\epsilon = 0.5$, ramification $r = 7$, and two values of temperature, $k_B T/\epsilon = 0.25$ (black) and 0.15 (red). A cycle-2 orbit can be graphically found as the solution of $\rho = f \circ f(\rho)$ with $\rho \neq f(\rho)$. This orbit represents modulated phases, with density oscillations along the generations of the tree (as illustrated in figure 1b). The orbit of period 2 can also be visualized by means of a cob-web plot, which we show as the blue dotted line in figure 5b. Note that the instability threshold occurs at the same point as the emergence of the stable cycle-2 phase, and that any fixed point located between the solutions of a stable cycle-2 orbit will be unstable. A numerical inspection of f and f_∞ leads to no additional structures of the map beyond these two scenarios.

In figure 6a we plot phase diagrams in terms of $(\mu + \delta)/|\Delta|$ and $k_B T/|\Delta|$, with $\Delta > 0$, in the mean-field limit (black line) and for a tree of finite ramification (red lines), using the interactions parameters of A_0 in the cubic diagram of Fantoni and collaborators [11]. Since there is a coincidence between stability and transition thresholds, we can use Eq. (10) to derive parametric equations for the critical line of the mean-field map,

$$\frac{k_B T}{|\Delta|} = \rho(1 - \rho), \quad (16)$$

and

$$\frac{\mu + \delta}{|\Delta|} = \rho(1 - \rho) \ln \frac{1 - \rho}{\rho} - \rho. \quad (17)$$

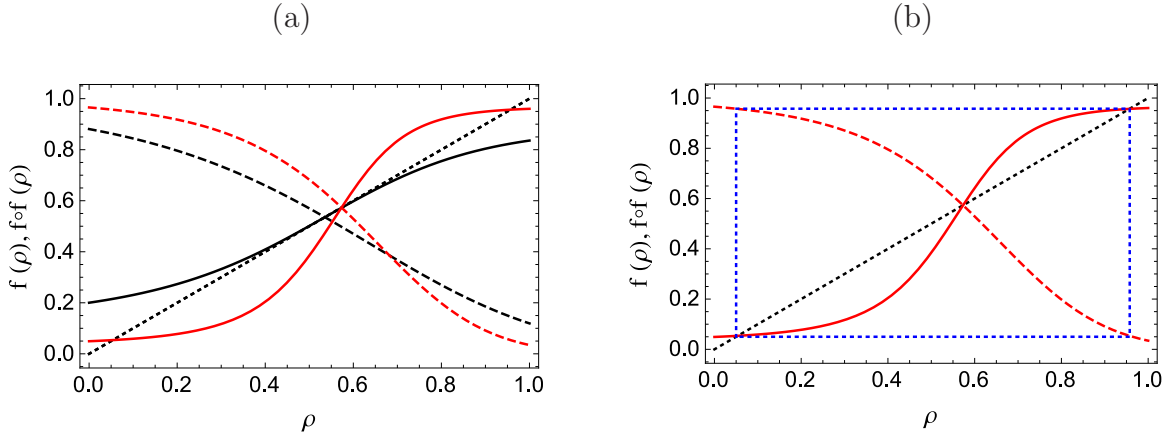


Figure 5. (a) Plots of ρ (dotted line), $f(\rho)$ (dashed lines), and $f \circ f(\rho)$ (solid lines), for fixed chemical potential, $\mu/\epsilon = 0.5$, ramification $r = 7$, and two values of temperature, $k_B T/\epsilon = 0.25$ (black) and 0.15 (red). A cycle-2 orbit can be graphically found as the solution of $\rho = f \circ f(\rho)$ with $\rho \neq f(\rho)$. (b) Cobweb plot to illustrate the period-2 cycle.

Note that the minus sign in the second term on the r.h.s. of this last equation is responsible for both the “soft” behavior near $k_B T/|\Delta| = 0.25$, and the reentrant behavior at low temperatures. For trees of finite coordination, we resort to a simple numerical calculation to find the analogous critical line. In figure 6b we plot the corresponding phase diagram in terms of ρ and $k_B T/|\Delta|$. As we mentioned above, there is no indication of an alternative critical behavior in the region enclosed by the critical line.

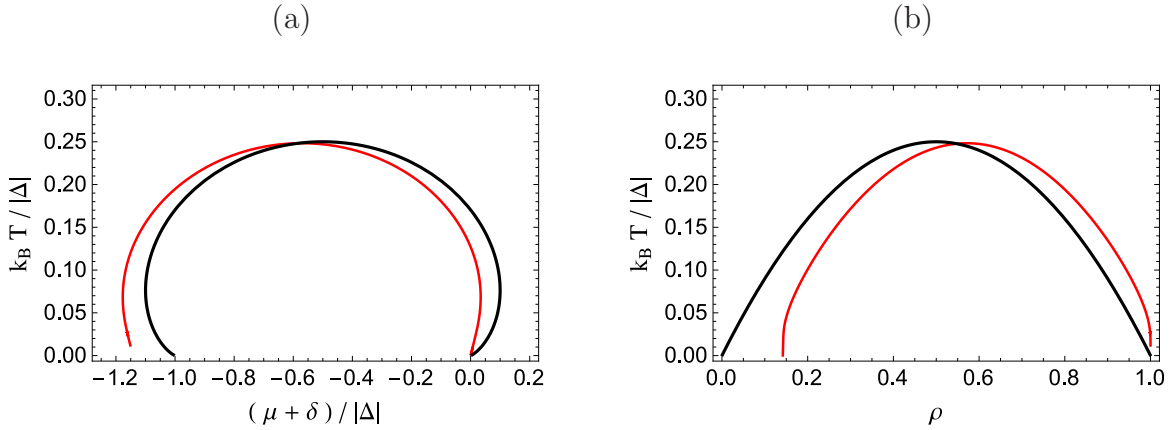


Figure 6. (a) Critical lines in the phase diagram in terms of temperature and chemical potential (with $\Delta > 0$). Red lines are for a tree of finite coordination. Black lines are obtained in the infinite-coordination limit. There is a modulated phase, of period 2, inside the region enclosed by the critical line. (b) Corresponding phase diagram in the $\rho \times T$ plane.

5. Duality and low coordination limit

We have found an interesting (dual) relation between the solutions for a cycle-2 orbit along a symmetry line and the phase-separated densities along the coexistence curve. Consider the mean-field map with $\Delta > 0$, so that at $(\mu + \delta)/|\Delta| = -1/2$, and $k_B T/|\Delta| < 1/4$, there is a periodic solution of the form $(\rho, 1 - \rho)$. Thus, we can write

$$1 - \rho = f_\infty(\rho) = \left[1 + e^{-(1-\rho)/2\tilde{T}}\right]^{-1}, \quad (18)$$

from which we have

$$\rho = \left[1 + e^{(1-\rho)/2\tilde{T}}\right], \quad (19)$$

where \tilde{T} is a short-hand notation for $k_B T/|\Delta|$. Hence, the solutions for the density along the coexistence curve for $\Delta < 0$ are identical to the periodic orbit solutions along the $(\mu + \delta)/|\Delta| = -1/2$ symmetry line for $\Delta > 0$.

We now consider the effects of the finite coordination of the tree on the critical properties of the two-state Janus gas. Let us restrict the attention to two representative cases of the cubic diagram of interactions, I_0 and A_0 , for $\Delta < 0$ and $\Delta > 0$, respectively. In the I_0 case, for $(\mu + \delta)/|\Delta| = 1/2$ and $\rho = 1/2$, we have

$$f'(\rho)|_{\rho=1/2} = r \tanh\left(\frac{|\Delta|}{4r k_B T}\right), \quad (20)$$

so that, at the critical point,

$$\frac{1}{r} = \tanh\left(\frac{|\Delta|}{4r k_B T_c}\right). \quad (21)$$

As it should be anticipated, $T_c = |\Delta|/4k_B$ is a trivial solution for the map in the mean-field limit ($r \rightarrow \infty$). Also, Eq. (21) has no solutions for $r < 1$, so $T_c \rightarrow 0$ as $r \rightarrow 1$. This result is consistent with the one-dimensional chain structure of the Bethe lattice for $r = 1$, since no transition is expected in one-dimensional systems with short-range interactions. Similar results can be obtained in the A_0 case (with $(\mu + \delta)/|\Delta| = -1/2$). We remark that the symmetry line of the mean-field map is shifted to the left as r is decreased, and the solution $\rho = 1/2$ at the critical point is no longer valid for finite r if we fix $(\mu + \delta)/|\Delta| = -1/2$. For finite ramification, we have to numerically calculate the value of ρ at the critical temperature.

6. Conclusions

We have considered a lattice gas of two-state Janus particles on the sites of a Cayley tree. Taking advantage of the geometrical structure of this graph, it is particularly simple to introduce directional interactions between first-neighbor sites along the branches of the tree. The problem is formulated in terms of a set recursion relations, whose attractors correspond to physical solutions on the Bethe lattice (the deep interior of the Cayley tree). With relatively easy calculations, we can draw a number of phase diagrams

in terms of temperature and either chemical potential or the concentration of a type of particles, and for a wide range of energy parameters. We then make contact with recent simulations for the analogous system of hard spheres with a short-range attractive potential well. The results on the Bethe lattice provide a unified view of the systems represented in a cubic diagram of interactions drawn by Fantoni and collaborators [11, 10]. In particular, depending on a combination of energy parameters, which includes the analog of the directional Kern-Frenkel potential, we show the existence of a critical line separating disordered and cycle-2 modulated phases, which have been found in some of the simulations for equal concentrations. The calculations on the Bethe Lattice are simple enough to give qualitative results for all choices of parameters of the model.

Acknowledgement

We acknowledge the financial support provided by the Brazilian agencies CNPq and Fapesp.

Appendix A. Derivation of recursion relations

In figure A1, we draw the configurations that are associated with two generations of a Cayley tree of ramification $r = 2$ (corresponding to coordination $q = r + 1 = 3$). This tree is constructed along a direction that leads to a consistent and unambiguous choice of the interaction parameters. We assume that a and b particles interact with energy $-\epsilon_{ab}$ if a particle of type a is on a site belonging to a certain generation and a particle of type b is on a nearest-neighbor site belonging to the next generation (and vice versa). There is a Boltzmann factor associated with each interaction between j and $j + 1$. There is also a fugacity term related to particles of type a ($t_{j+1} = 1$). For this 3-coordinated tree, let Ξ_j^a (Ξ_j^b) be the partial grand partition function associated with the sub-tree generated by a site at generation j which is occupied by a particle of type a (b). Thus, the partial partition functions at generations j and $j + 1$ obey the set of relations

$$\Xi_{j+1}^a = z \left[e^{2K_{aa}} \left(\Xi_j^a \right)^2 + 2e^{K_{aa}+K_{ab}} \left(\Xi_j^a \Xi_j^b \right) + e^{2K_{ab}} \left(\Xi_j^b \right)^2 \right] \quad (\text{A.1})$$

and

$$\Xi_{j+1}^b = e^{2K_{ba}} \left(\Xi_j^a \right)^2 + 2e^{K_{ba}+K_{bb}} \left(\Xi_j^a \Xi_j^b \right) + e^{2K_{bb}} \left(\Xi_j^b \right)^2, \quad (\text{A.2})$$

where $K_{kl} = \beta \epsilon_{kl}$, for $k, l = a, b$, $\beta = 1/k_B T$ is the inverse temperature, $z = \exp(\beta \mu)$ is the fugacity, and μ is the chemical potential (associated with particles of type a). For a tree with a general ramification r , we have the more general equations

$$\Xi_{j+1}^a = z \left[e^{K_{aa}} \Xi_j^a + e^{K_{ab}} \Xi_j^b \right]^r \quad (\text{A.3})$$

and

$$\Xi_{j+1}^b = \left[e^{K_{ba}} \Xi_j^a + e^{K_{bb}} \Xi_j^b \right]^r. \quad (\text{A.4})$$

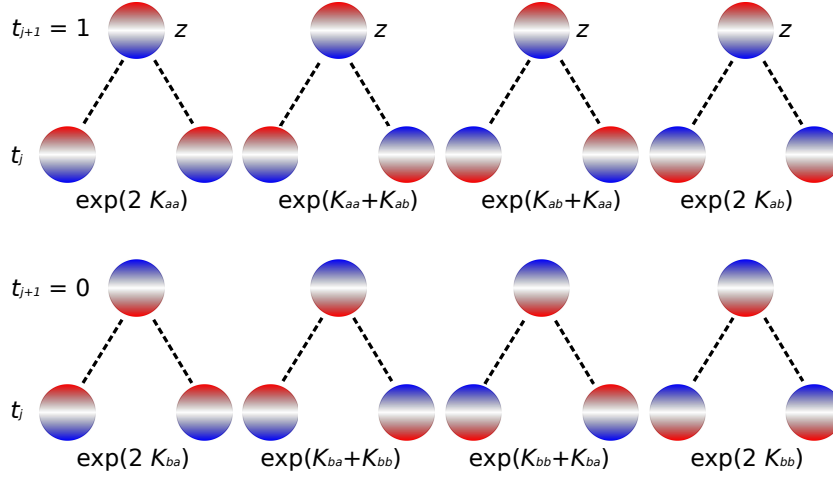


Figure A1. Illustrations of the possible configurations at the j -th generation with $t_{j+1} = 1$ (top) and $t_{j+1} = 0$ (bottom). Note that we write the Boltzmann factor associated with each configuration. A fugacity term z is present at the recursion relation if $t_{j+1} = 1$.

References

- [1] S. Jiang and S. Granick. *Langmuir*, 24:2438, 2008.
- [2] S. Gangwal, A. Pawar, I. Kretzschmar, and O. D. Velez. *Soft Matter*, 6:1413, 2010.
- [3] A. Reinhardt, A. J. Williamson, J. P. K. Doye, J. Carrete, L. M. Varela, and A. A. Louis. *J. Chem. Phys.*, 134:104905, 2011.
- [4] T. Vissers, Z. Preisler, F. Smalenburg, M. Dijkstra, and F. Sciortino. *J. Chem. Phys.*, 138:164505, 2013.
- [5] S. Jiang, J. Yan, J. K. Whitmer, S. M. Anthony, E. Luijten, and S. Granick. *Phys. Rev. Lett.*, 112:218301, 2014.
- [6] H. Shin and K. S. Schweizer. *Soft Matter*, 10:262, 2014.
- [7] N. Kern and D. Frenkel. *J. Chem. Phys.*, 118:9882, 2003.
- [8] F. Sciortino, A. Giacometti, and G. Pastore. *Phys. Rev. Lett.*, 103:237801, 2009.
- [9] F. Sciortino, A. Giacometti, and G. Pastore. *Phys. Chem. Chem. Phys.*, 12:11869, 2010.
- [10] M. A. G. Maestre, R. Fantoni, A. Giacometti, and A. Santos. *J. Chem. Phys.*, 138:094904, 2013.
- [11] R. Fantoni, A. Giacometti, M. A. G. Maestre, and A. Santos. *J. Chem. Phys.*, 139:174902, 2013.
- [12] L. K. Runnels. *J. Math. Phys.*, 8:2081, 1967.
- [13] J. C. Thompson. *J. Stat. Phys.*, 27:441, 1982.
- [14] R. J. Baxter. *Exactly solved models in statistical mechanics*. Academic Press, London, 1982.